Position-Force Domain Passivity of the Human Arm in Telerobotic Systems*

Mahya Shahbazi, *Member, IEEE,* Seyed Farokh Atashzar, *Member, IEEE,* Mahdi Tavakoli, *Member, IEEE,*
Rajni V. Patel, *Life Fellow, IEEE*

Abstract—In order to guarantee safe human-robot interaction in single-master/single-slave teleoperation systems, passivity-based controllers have traditionally been developed for communication delay compensation in the *velocity-force domain* with the assumption of passivity of the human arm. The same controllers can also make the delayed communication channel passive in the *position-force domain*, which provides a convenient position-drift-free control strategy for more complicated scenarios such as multi-master/single-slave systems. This would, however, only work if the operator's arm also remains passive in the position-force domain. Whether the arm remains passive in the position-force domain is a critical question yet to be answered. In this paper, passivity of the human arm in the position-force domain is investigated through mathematical analysis, experimentation and statistical user studies involving 12 subjects and 48 trials. It is shown that unlike in the velocity-force domain, the human operator will not remain passive in the position-force domain for all frequency ranges. This implies the need for appropriate control strategies to make the human operator termination passive in the position-force domain. For future design of suitable controllers, statistical analyses are performed to investigate correlations between the levels of position-force domain passivity of the left and the right arms of the human participants, as well as the levels of passivity of the subjects' arms and their physical characteristics, e.g., weight, height, and body mass index. Possible control strategies through which the passivity of the operator termination can be guaranteed are also discussed.

Keywords– *Passivity-Based Controller, Position-Force Domain Passivity, Arm Passivity, Teleoperation, Telerobotics.*

I. INTRODUCTION

Teleoperation extends an operator's sensing and manipulation capabilities to a remote location. It facilitates off-site robotic performance of a desired task through a user console, and ensures cost-effectiveness, safety and accessibility. Teleoperation systems have been broadly used in a wide range of

M. Shahbazi and S.F. Atashzar are with Canadian Surgical Technologies and Advanced Robotics (CSTAR), and with the Department of Electrical and Computer Engineering, Western University, London, ON, Canada. They were also visiting research scholars at the University of Alberta, Edmonton, AB, Canada (email: mshahba2@uwo.ca, satashza@uwo.ca). M. Tavakoli is with the Department of Electrical and Computer Engineering, University of Alberta, Edmonton, AB, Canada (email: mahdi.tavakoli@ualberta.ca). R.V. Patel is with CSTAR, the Department of Electrical and Computer Engineering, the Department of Clinical Neurological Sciences, and the Department of Surgery, Western University (email: rvpatel@uwo.ca).

applications from mining to space and underwater exploration to robotics-assisted minimally invasive surgery [1], [2], robotic surgical training [3], [4], and robotics-assisted rehabilitation therapy [5], [6]. A teleoperation system consists of three main components: 1) A slave robot, performing a desired task on a designated environment, 2) a master console manipulated by an operator, remotely controlling the slave console; and 3) a communication channel to transmit data between the master and the slave [7]. Fig. 1 shows the overall scheme of a single-master/single-slave teleoperation system, in which teleoperator refers to the set of communication channels integrated with the master and the slave robots. Long-distance communication can introduce time delays into the system, which can cause instability [8]. To ensure robust stability of the system against communication delays in order to guarantee safe human-robot interaction, passivity-based control methodologies have been developed building on the following passivity theorems:

Theorem I: A system is passive if it consists solely of passive elements [9].

Definition I: A general time-varying n-port network with zero initial energy storage is passive if [10], [11]:

$$\varepsilon(t) = \int_0^t U^T(\tau) \cdot Y(\tau) \, d\tau \geq 0 \qquad (1)$$

where $U \in R^n$ and $Y \in R^n$ correspond to the input and output of the network, respectively.

Based on *Theorem I* and by the assumption of passivity of the operator and the environment [12], [13], the only element to make passive is the teleoperator (which is equivalent to making the communication channel passive), for which several methodologies have been introduced in the literature. These approaches can be classified into two main categories: 1) Time Domain Passivity Controller (TDPC) [14], [15], and 2) Frequency Domain Passivity Controller (FDPC), which includes Scattering Matrix [16] and Wave Variables [17] approaches.

According to *Definition I*, passivity of a general system can be analyzed based on the input and output of the system, regardless of their nature. In the teleoperation systems literature, all of the existing approaches have addressed the passivity of the communication channel (and therefore, the passivity of the teleoperator) by considering the Input-Output (IO) pair to be

Fig. 1: The overall scheme of a teleoperation system. The teleoperator includes the communication channel as well as the master and the slave robots. $U = [u_1, u_2]$ and $Y = [y_1, y_2]$ refer to the input and output of the teleoperator, respectively.

velocity and force signals. This has imposed the limitation of having to transmit the velocity signal from the master side to the slave side, rather than transmitting the position signal. Transmission of the velocity signal causes position-error accumulation and position drift, which considerably degrades the position tracking performance of the system [14].

Several techniques have been proposed in the literature in order to address the position drift caused by the FDPCs [18], [19], [20], and a few methods were recently proposed to compensate for the position drift in TDPC systems [14], [21]. However, these approaches, which mostly modify the conventional passivity controllers, have been mainly developed for addressing the position drift in bilateral Single-Master/Single-Slave (SM/SS) teleoperation systems, and are not straight-forwardly applicable to a Multi-Master/Single-Slave (MM/SS) framework, due to the topographical complexities of MM/SS platforms. MM/SS systems have been shown to be useful in supervised robotics-assisted surgical training [3], [4] and rehabilitation [22], [23], where an expert surgeon/therapist can be directly involved in the procedure based on haptic interaction with a trainee/patient. According to a recent study [24], haptics-based interaction with a partner when learning a motor task considerably enhances motor skills compared to when practicing the task alone for the same duration.

Considering the mathematics behind most of the *conventional* passivity controllers proposed in the literature for SM/SS systems, which is fundamentally based on (1), the same controller that makes the communication channel passive for the IO pair of force and velocity (i.e., Velocity-force Domain (VD)) can also make the channel passive for the IO pair of force and position (i.e., Position-force Domain (PD)). This immediately addresses the position-drift issue and may be straightforward to apply not only to SM/SS systems, but also to more complex frameworks such as MM/SS and Multi-Master/Multi-Slave (MM/MS) systems. Although using a PD controller to make the communication channel passive is possible through the existing passivity-based approaches, according to Fig. 1, it necessitates the connection terminal of the operator-teleoperator[1] to also remain passive in the PD in order to comply with *Theorem I*. For this purpose, passivity of the operator terminal in the PD, however, is a critical question to be investigated. In fact, passivity of the operator in the VD seems to be the main reason behind the development of all the passivity-based controllers to date in the VD. While there have been a number of studies on the numerical measurement of the endpoint impedance of the arm [25], [26], [27], there are very few studies on PD Passivity (PDP) of the operator. In [28], PD passivity of the human arm was assessed through numerical measurement of the endpoint impedance of the arm. The assessment has been performed over a limited range of frequency and does not discuss the frequency-dependence of PD passivity.

Therefore, to facilitate PDP controllers for teleoperation systems regardless of the complexity of the framework and the number of master and slave robots involved, the main question

to answer is whether the operator is passive in the position-force domain as well; and if not, what measures should be taken in order to make the operator termination passive. Consequently, in this paper, the PDP of the human operator has been investigated through mathematical and experimental analyses as well as statistical user studies involving 12 subjects and 48 trials. It has been shown that, unlike in VD, the operator will not remain passive in PD for all frequency ranges; This implies the need for appropriate control strategies to make the human operator termination passive in PD. For future design of suitable controllers, statistical analyses are conducted to investigate the possible correlation between the levels of PD passivity of the left and right arms of the human participants, and the levels of passivity of the subjects' arms and their physical characteristics, e.g., weight, height, and body mass index. Possible control strategies through which the passivity of the operator termination can be ensured are also discussed.

The rest of the paper is organized as follows: Section II analyzes passivity of the operators in PD, mathematically. Section III gives experimental results in support of the mathematical analysis. Section IV discusses the user trials on humans, and statistically analyzes PD passivity as well as correlations between the subjects' physical features and passivity levels of their arms. Section V suggests possible control approaches to ensure the PDP of the operator termination. Section VI provides a case study on implementation of the proposed control approaches on a bilateral SM/SS teleoperation system and Section VII concludes the paper.

Remark I: *Besides passivity-based controllers (which have been mostly developed in VD), there also exist other control methodologies for teleoperation systems. Examples of such controllers include [29], [30], which have been developed based on Input-to-Output Stability (IOS) and Input-to-State Stability (ISS) analyses. Passivity-based vs. ISS/IOS-based controllers are both valuable methodologies and have their advantages and disadvantages. The focus of the current paper, however, is to open up a new perspective to design and implementation of passivity controllers directly in the position-force domain, and detailed comparison of passivity controllers with non-passivity approaches is out the scope of this paper.*

II. MATHEMATICAL ANALYSIS

The dynamics of the human arm can be modeled by a second-order system [31]:

$$M_h\ddot{x}_h(t) + B_h\dot{x}_h(t) + K_h(x_h(t) - x_{h_0}) = f_h(t) \qquad (2)$$

Here, f_h refers to the force applied to the arm endpoint, x_h is the hand position, and x_{h_0} is the hand equilibrium position commanded by the Central Nervous System (CNS)[2]. In addition, M_h, B_h and K_h denote the constant real-valued inertia, damping and stiffness of the arm. By the change of variables $x = x_h - x_{h_0}$, (2) is transformed to:

$$M_h\ddot{x}(t) + B_h\dot{x}(t) + K_hx(t) = f_h(t) \qquad (3)$$

---

[1]"Connection terminal of the operator-teleoperator" refers to the terminal through which the operator is connected to the teleoperator.

[2]Hand equilibrium position can be interpreted as the desired reference for the human intention, which is gradually shifted by the CNS between the movement end-points in order to control the arm movement [25], [32].

where x refers to the displacement with respect to the equilibrium point x_{h_0}. Taking the Laplace transform of (3) yields

$$(M_h s^2 + B_h s + K_h)X(s) = F_h(s) \qquad (4)$$

where $F_h(s) = \mathscr{L}\{f_h(t)\}$ and $X(s) = \mathscr{L}\{x(t)\}$, in which $\mathscr{L}$ and s indicate the Laplace operator and the Laplace variable, respectively. Continuing the analysis in one Degree-Of-Freedom (DOF) in the interest of simplicity and without loss of generality, the admittances of the human arm in the position-force domain, $Y_P(s)$, and in the velocity-force domain, $Y_V(s)$ can be written as follows:

$$Y_P(s) = \frac{X(s)}{F_h(s)} = \frac{1}{M_h s^2 + B_h s + K_h} \qquad (5)$$

$$Y_V(s) = \frac{V(s)}{F_h(s)} = \frac{s}{M_h s^2 + B_h s + K_h} \qquad (6)$$

where $V(s) = \mathscr{L}\{v(t)\}$ and $v(t) = \dot{x}(t)$.

In order for a transfer function $G(s)$ to represent a passive system, $G(s)$ must be Positive Real (PR) [33][3]. Investigate the positive-realness and therefore the passivity of the human arm in the velocity-force domain, and considering that M_h, B_h and K_h have positive values, yields:

$$Y_V(jw) + Y_V(-jw) = \frac{2B_h w^2}{(K_h - M_h w^2)^2 + (B_h w)^2} \geq 0 \qquad (7)$$

which is always true, as B_h refers to a positive-valued damping term. Therefore, $Y_V(s)$ satisfies the PR criteria, which implies the passivity of the human arm with respect to the force-velocity input-output pair. This is completely in agreement with the literature, where the human arm has been considered passive for *force-velocity* interactions [12].

Investigating the PR criteria condition for $Y_P(s)$ leads to

$$Y_P(jw) + Y_P(-jw) = \frac{2(K_h - M_h w^2)}{(K_h - M_h w^2)^2 + (B_h w)^2} \geq 0 \qquad (8)$$

which is dependent not only on K_h and M_h, but also on the frequency w, and is not true for $w > w_n = \sqrt{\frac{K_h}{M_h}}$. Therefore, unlike in the VD, the human arm does not remain passive in the PD for all frequency ranges.

Remark II: *Giving the analysis in one DOF does not affect generality, as the above serves as a counterexample to show the non-passivity of the operator in the position-force domain. The same applies to the posture-independent and time-invariant second-order model considered for the human arm in (2). Although this model is a simplified model of the human arm's neuro-musculoskeletal structure as detailed in [31], it can still show the position-force domain non-passivity of the human arm as opposed to the velocity-force domain, even for the simplest model. Moreover, in order to analyze the PD passivity of the human arm without forgoing the analysis accuracy as a result of unmodelled dynamics and uncertainties, user trials and statistical analysis involving human operators have*

been also conducted as detailed in Section IV. The analysis given in Section IV relies on the passivity measure, which is input/output-dependant, rather than model-dependant, and addresses concerns with thoroughness of the dynamic model considered for the arm."

What can be inferred from (8) is that increased stiffness of the arm can contribute to the PD passivity of the arm, while the arm's inertia has an active effect. Moreover, the higher the motion frequency, the higher the possibility of non-passivity. In order to further evaluate these findings, experiments were conducted as described in the following section.

III. EXPERIMENTAL ANALYSIS

In order to investigate the passivating[4] or non-passivating effect of inertia, stiffness and motion frequency, experiments were conducted. The experimental setup, shown in Fig. 2, consists of an adjustable custom-built Mass-Spring Array (MSA) connected to a 2-DOF planar Quanser rehabilitation robot (Quanser Consulting Inc., Markham, ON, Canada). The capstan drive mechanism of the Quanser rehabilitation robot makes it back-drivable with low friction and inertia. The robot is capable of exerting forces up to 50 N throughout its semicircular workspace, and the motors encoders provide a resolution of better than 0.002 mm in Cartesian space [28]. The modular structure of the MSA allows us to add external mass and spring elements to examine the effect of various inertia/stiffness values. During the experiments conducted in three scenarios, the MSA's end-point was perturbed by the robot using the following Persistently Exciting (PE) perturbation:

$$P = 0.0025 \cdot \sum_{k=1}^{4} \sum_{j=1}^{3} \sin\left(\frac{w_j t}{k}\right) \qquad (9)$$

where $w_1 = 1.2\pi$, $w_2 = 2\pi$, and $w_3 = 3\pi \frac{rad}{s}$. The position of the MSA's endpoint, x_{MSA}, and the force applied to the MSA, f_{MSA}, were measured in 2 Cartesian directions along X and Y axes. In order to measure f_{MSA}, an ATI Gamma force sensor (ATI Industrial Automation Inc., Apex, NC, USA) was placed between the robot's End-Effector (EE) and the MSA. The force sensor has a resolution of 0.0125 N and maximum measurable force of 65 N along X-Y axes. Since the robot's EE was in contact with the MSA's end-point, the position and velocity of the robot's EE captured by applying forward kinematics to the robot's joint positions reading served as those of the MSA's end-point (x_{MSA} and v_{MSA}).

The PD passivity of the MSA system in each experimental trial was investigated using Definition I with respect to force-position input-output pair by checking if:

$$\varepsilon_{PD}(t) = \int_0^t x_{MSA}^T(\tau) \cdot f_{MSA}(\tau) \, d\tau \geq 0 \qquad (10)$$

Note that MSA was relaxed at $t = 0$, so the initial energy was zero, and therefore the passivity condition given in (10) was checked with the right-hand side being zero.

Remark III: *The experiments were designed in such a way that each scenario investigates the effect of one single*

---

[3]The definition of a PR transfer function has not been included in the interest of the space, and can be found in [34].

[4]The term "passivate" has been used as a synonym for "make passive".

parameter over the PD passivity at a time. This allows to examine the correlation of the PD passivity with each parameter independently, without superimposing multiple effects on the correlation outcome.

A. Experimental Scenario I

The first experiment was conducted for a series of mass values, namely, $m_1 = m_0$, $m_2 = m_0 + 0.230kg$, $m_3 = m_0 + 0.460kg$, and $m_4 = m_0 + 0.690kg$ by adding masses to the system, with no springs added; $m_0 > 0$ refers to the mass of the handle between the force sensor and the MSA before adding any external mass to the MSA. Fig. 3a shows ε_{PD} calculated for the mass values. As can be seen in this figure, ε_{PD} for all m_i $(i = 1, 2, 3, 4)$ has negative and decreasing value for all $t \geq 0$, which indicates non-passivity of the mass. As can also be seen in this figure, the heavier the mass, the more non-passive behavior it shows, which is in agreement with the mathematical analysis discussed in the previous section.

B. Experimental Scenario II

The second experiment investigates the effect of stiffness on passivity. For this purpose, stiffness elements were added to the same mass values m_i $(i = 1, 2, 3, 4)$ as in previous scenario by adding a set of springs ($k_1 = 50$, $k_2 = 175$, $k_3 = 190$, $k_4 = 230 \frac{N}{m}$) to the MSA. Fig. 3b shows ε_{PD} calculated for the sets of mass-spring elements. Comparing Fig. 3b with Fig. 3a, the passivating effect of stiffness components as opposed to mass components can be seen. Although m_i $(i = 1, 2, 3, 4)$ moves the system towards non-passivity (as shown in Fig. 3a), adding stiffness can reverse the trend and make the system passive. This result is also in agreement with the PD passivity condition derived in the previous section.

C. Experimental Scenario III

Considering the passivity condition given in (8), in addition to mass and stiffness, motion frequency can also play an
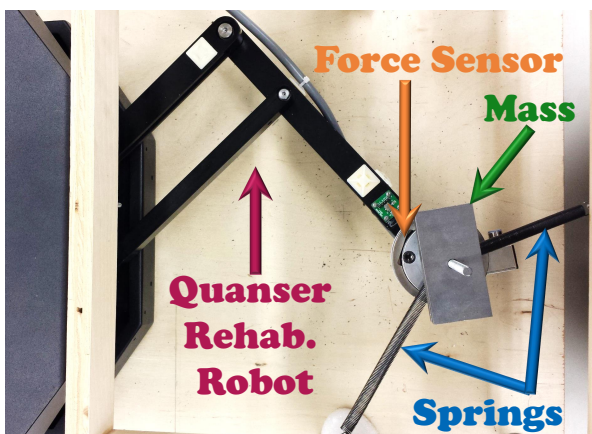

Fig. 2: The mass-spring array system connected to the 2-DOF planar Quanser rehabilitation robot.

essential role in passivity of the arm in PD. Therefore, a third experiment is designed to examine the effect of the perturbation's frequency range. For this purpose, experimental scenario I has been repeated for the same circumstances, including the mass values, except for the frequency range of the perturbation signal. In this experiment, the perturbation given in (9) has been applied for $w_1 = 2\pi$, $w_2 = 6\pi$, and $w_3 = 10\pi \frac{rad}{s}$. Fig. 3c shows ε_{PD} calculated for the mass elements perturbed at higher frequencies. Comparing Figs. 3a and 3c, it can be seen that, although the mass elements have shown non-passive behavior in both frequency ranges (experimental scenario I and III), the rate of non-passivity was considerably higher for the higher-frequency perturbation (experimental scenario III). In 60 seconds, ε_{PD} has reached from 0 to -0.045 for the low-frequency perturbation (Fig. 3a), while during the same time ε_{PD} for the high-frequency perturbation has dropped from 0 to -1.54 (Fig. 3a).

The experimental results in this section support the mathematical analysis given in Section II. As verified in both Sections II and III, stiffness can contribute towards passivity in PD, while mass and increased frequency work against passivity of the arm in the position-force domain. The analyses given in Sections II and III build upon the second-order model approximation for the human arm. Although the model is very popular in the literature and has been used to a large extent, there still might be a question of accuracy due to the unmodeled dynamics. To address concerns about the thoroughness of the model, a series of user trials has also been conducted as discussed in the following section.

IV. USER TRIALS AND STATISTICAL ANALYSIS

In order to analyze the PD passivity of the human arm without forgoing the analysis accuracy as a result of possible model reduction/uncertainty in the previous section, user trials were conducted.

A. Subjects

Twelve healthy subjects (5 women, 7 men; mean age, 29 years; age range, 26-40 years) were recruited. Data was collected for both left and right arms of the subjects, giving us 24 sets of data. Two participants were left-handed and 10 right-handed, all with no history of motor impairment. All participants gave written informed consent to participate in the study. The study was approved by the Research Ethics Board (REB) at the University of Alberta.

B. Setup and Procedure

As illustrated in Fig. 4, each subject sat in front of a Quanser rehabilitation robot and grasped the robot's handle with their hand. They were asked to relax their arm and avoid voluntary intervention as the robot applied perturbations to their arm. All data was collected at test locations in which the subject's forearm formed a right angle with their upper-arm in the interest of consistency. Each trial was repeated four times for each subject, collecting force and position data on
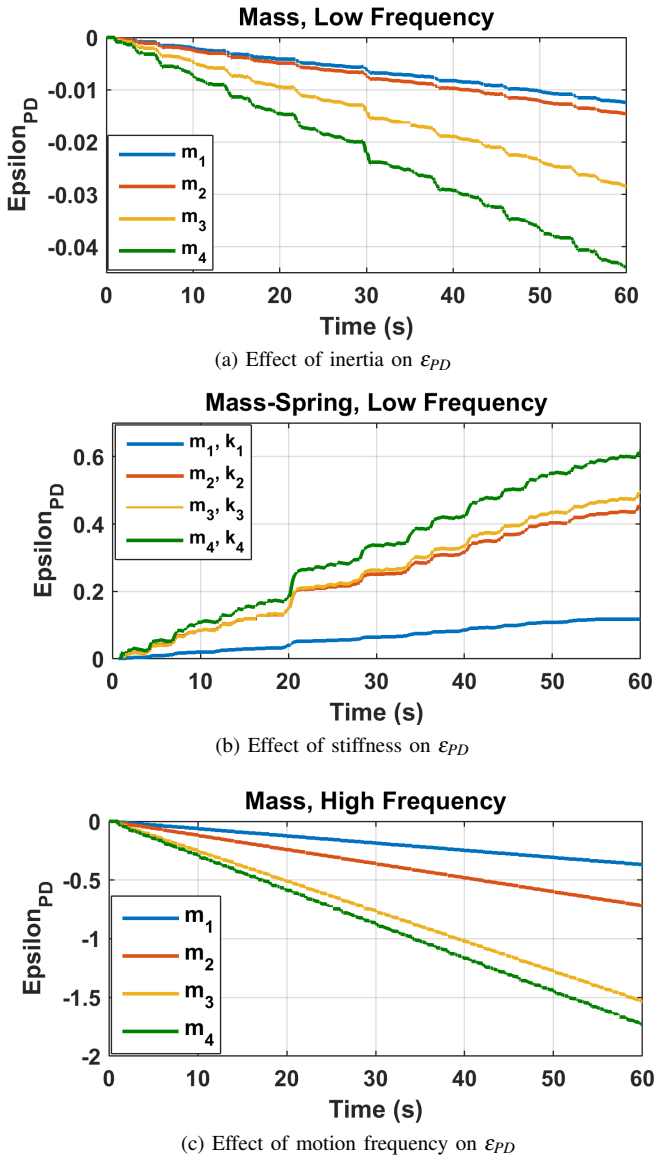
(a) Effect of inertia on ε_{PD}

(b) Effect of stiffness on ε_{PD}

(c) Effect of motion frequency on ε_{PD}

Fig. 3: Experimental results

Fig. 4: The experimental setup used in the user trials.

both right and left arms with two different frequency ranges of perturbations applied to each side for two minutes. The following PE position perturbation signals were applied to the subject's hand in X and Y directions:

$$P_X = 0.015. \sum_{k=1}^{4} \sum_{j=1}^{3} sin(\frac{w_j t}{k}) sin(\theta t)$$
$$P_Y = 0.015. \sum_{k=1}^{4} \sum_{j=1}^{3} sin(\frac{w_j t}{k}) cos(\theta t) \tag{11}$$

In (11), w_1, w_2, w_3, θ are respectively set to 0, π, 2π and $0.55\pi \ \frac{rad}{s}$ for the lower range of perturbation frequencies, and to 3π, 6π, 12π and $0.35\pi \ \frac{rad}{s}$ for the higher range of perturbation frequencies. The low and high ranges of perturbation frequencies were selected based on a threshold calculated according to the natural frequency of a typical
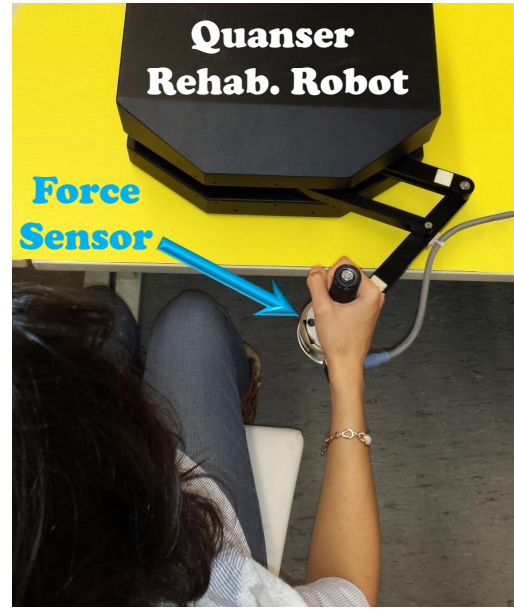
human arm. For this purpose, a stiffness of $K_h = 100 \frac{N.s^2}{m}$ and a mass of $M_h = 1Kg$ [28] were considered in (2) leading to a natural frequency as $w_n = \sqrt{\frac{K_h}{M_h}} = 3.2\pi \frac{rad}{s}$. This shows natural frequency based on the mathematics derived in Section II, may serve as the passivity/non-passivity threshold of the arm. The low-frequency signal was generated such that, while having a rich frequency content, its largest frequency remained below $3.2\pi \frac{rad}{s}$. The high-frequency perturbation signal was also generated such that it contained higher-than-threshold frequencies, while having a rich frequency content.

Note that the two-dimensional perturbation would suffice for the analysis of the relative contributions of the shoulder, elbow, and biarticular muscles to the overall limb passivity/activity, without entailing the experimental complexity of a full multi-dimensional evaluation [28] and [25].

During the trials, the forces applied by the subject's hand to the robot's end-effector was measured using the ATI Gamma force sensor located at the robot's EE. The position of the robot's EE also served as the position of the subject's hand endpoint, as the subjects were grasping the robot's handle. PD passivity of the subject's arm for each experimental trial was investigated using the general passivity criterion given in (1) with respect to force-position IO pair by calculating $\varepsilon_{PD}(t) = \int_0^t x_h^T(\tau) . f_h(\tau) \, d\tau$. It should be noted that using the general input-output-based criterion to investigate the system passivity eliminates any necessity for estimation of the human arm impedance parameters (mass, damping and inertia). Due to its model-free nature, the IO approach does not suffer from possible inaccuracies/uncertainties of various arm models.

C. Results

Figs. 5a, 5b, 6a and 6b illustrate ε_{PD} calculated for the subject during the following four sets of trials, respectively;

1) LH-LF: Left Hand, Low-Frequency perturbation; 2) RH-LF: Right Hand, Low-Frequency perturbation; 3) LH-HF: Left Hand, High-Frequency perturbation; and 4) RH-HF: Right Hand, High-Frequency perturbation.

1) Passivity/Non-passivity in Low-Frequency Trials: As it can be seen in Figs. 5a and 5b, ε_{PD} remained positive for both right and left arms of the subjects during the low-frequency trials. This indicates passivity of the subjects' arms during the low-frequency trials. However, it can also be seen that subject #10 had a fluctuating ε_{PD} with growing oscillations, which could have caused negative ε_{PD} if the trials had lasted longer. Therefore, despite its positive ε_{PD}, we consider the behavior of subject #10 as non-passive. Oscillations can also be seen in the ε_{PD} calculated for subject #5 in the LH-LF trial and subjects #7 and #8 in the RH-LF trial. However, the damped nature of those oscillations eliminates the possibility of ε_{PD} getting non-passive in the long run.

In order to investigate the statistical significance of the result (passivity of the arm in low-frequency ranges), statistical analysis was conducted to illustrate that the high number of passive behaviors during RH-LF and LH-LF did not occur by chance. In this case, an occurrence possibility of 0.5 indicates equal chance of passivity/non-passivity for the subjects during the trials. Based on the high number of passive behaviors during RH-LF and LH-LF, we hypothesize the following:

Hypothesis: The real probability of passive behavior during low-frequency perturbations is greater than 0.5.

Based on this alternative hypothesis, the null hypothesis is defined as follows:

Null hypothesis: The real probability of passive behaviors in RH-LF and LH-LF trials is **not** greater than 0.5.

In order to examine this null hypothesis, a binomial test was carried out. A binomial test statistically compares the number of successes (the number of passive behaviors during RH-LF and LH-LF trials, i.e., 22), observed in the total number of trials, i.e., 24, with a hypothesized probability of success (that is hypothesized to be greater than 0.5).

Using the binomial test, the null hypothesis is rejected with *p-value* $= 1.794e - 05$, which is well below 0.05, indicating that the true possibility of passive behavior during low-frequency perturbation is significantly greater than 0.5 (The probability of passivity as given by the binomial test is 0.9166).

2) Passivity/Non-passivity in High-Frequency Trials: Figs. 6a and 6b illustrate ε_{PD} calculated for left and right arms of the subjects during the high-frequency trials, i.e., RH and LH, respectively. As can be seen in these figures, ε_{PD} had a negative decreasing trend during all the high-frequency trials, except for the right arm of subject #9. This negative ε_{PD} along with its decreasing trend indicates non-passivity of the subjects. This results is in agreement with the mathematics derived in Section II, which associates the higher chance of non-passivity to the higher range of movement frequencies.

The interesting point about the trend of ε_{PD} for subject #9 in the RH trial (Fig. 6b) is that, although it has shown a passive behavior, the level of passivity has decreased considerably compared to that in the RL trial (Fig. 5b). This also illustrates the non-passivating effect of the high-frequency perturbation on subject #9, although the perturbation frequency range has

TABLE I: Mean-value of the quantified passivity levels

LH-LF	RH-LF	LH-HF	RH-HF
0.0018	0.0017	-0.0040	-0.0039

yet been low enough for his right arm to behave passively.

In order to investigate the statistical significance of the result (non-passivity of the arm in high-frequency ranges), statistical analysis was conducted to indicate that the high number of non-passive behaviors during RH and LH did not occur by chance. Similar to the previous case, an occurrence possibility of 0.5 indicates equal chance of passivity/non-passivity for the subjects, based on which the hypothesis is defined, as follows:

Hypothesis: The real probability of non-passive behavior during high-frequency perturbations is greater than 0.5.

Based on this alternative hypothesis, the null hypothesis is defined as follows:

Null hypothesis: The real probability of non-passivity during the high-frequency perturbations is **not** greater than 0.5.

In order to examine this null hypothesis, a binomial test was carried out. Based on the results in Figs. 6a and 6b, the number of successes (that is the number of non-passive behaviors, in this case) was set to 23. The total number of trials was set to 24 and the hypothesized probability of success was set to be greater than 0.5.

Using the binomial test, the null hypothesis is rejected with *p-value* $= 1.49e - 06$, which is well below 0.05, indicating that the true possibility of non-passivity during high-frequency perturbation is significantly greater than 0.5 (The probability of non-passivity as given by the binomial test is 0.9583).

3) Passivity/Non-passivity Correlation Between Left and Right Arms: Figs. 7a and 7b compare ε_{PD} for left and right arms of two of the subjects in low-frequency and high-frequency trials, respectively. In both frequency ranges, correlations can be seen between the level of passivity/non-passivity of each subject's left and right arms. The level of correlation from one person to another could vary based on the mechanical properties of the person's arms such as muscle density and strength. By looking at the results in Figs. 5-6, it can be seen that not all of the subjects have shown similar passivity/non-passivity behavior between their left and right arms. In order to investigate the possible correlation between their left and right arms, statistical analysis was carried out. For this purpose, the slope of ε_{PD} calculated for the subjects' arms was used as a metric to quantify the degree of passivity/non-passivity in subject's arms. In order to calculate the average slope of ε_{PD} for each subjects' arms, the linear least-squares curve-fitting method was applied. The slope of the fitted straight-line was recorded for each ε_{PD} as a quantified passivity/non-passivity metric. Fig. 8 illustrates the quantified passivity/non-passivity degree for the subjects during the four trials.

Fig. 9a shows the distribution of the quantified data for all the subjects during the four sets of trials (LH-LF, RH-LF, LH-HF, RH-HF). The mean-value of the quantified passivity/non-passivity levels for all the trials are given in Table I. Fig. 9b also compares the distributions for the Left Hands (LH) and Right Hands (RH), disregarding the frequency range of
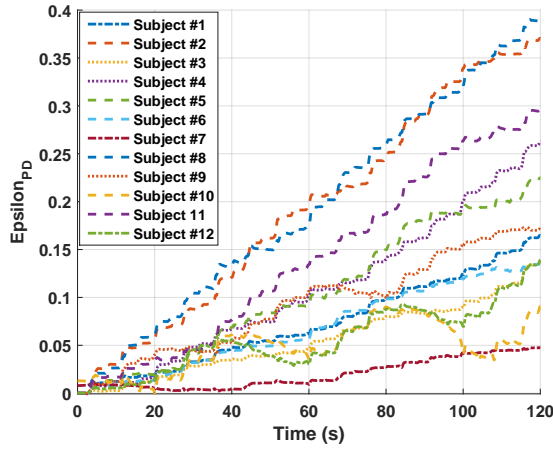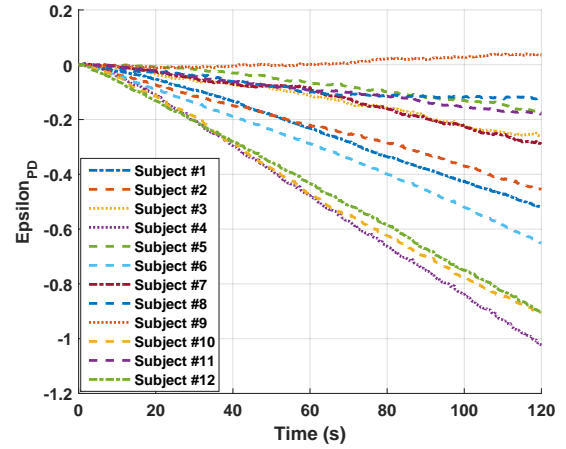
(a) ε_{PD} for the left hand of all of the subjects recorded during low-frequency perturbation
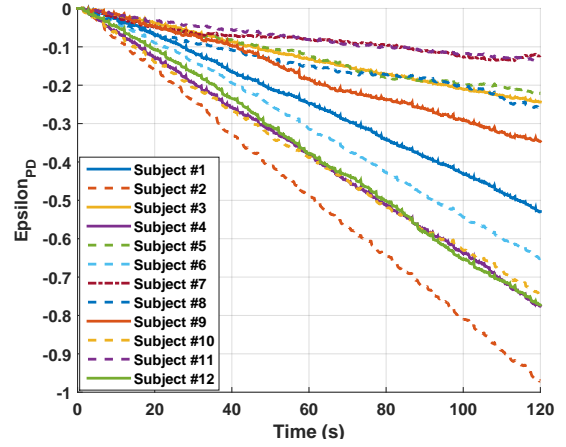
(b) ε_{PD} for the right hand of all of the subjects recorded during low-frequency perturbation
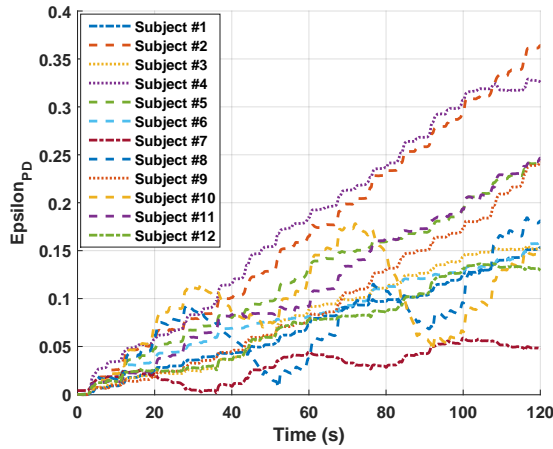
Fig. 5: ε_{PD} for all of the subjects recorded during low-frequency perturbation

(a) ε_{PD} for the left hand of all of the subjects recorded during high-frequency perturbation

(b) ε_{PD} for the right hand of all of the subjects recorded during high-frequency perturbation

Fig. 6: ε_{PD} for all of the subjects recorded during high-frequency perturbation

the perturbations. Both Figs. 9a and 9b indicate a reasonable correlation between the passivity/non-passivity level of the subjects' left and right arms.

In order to statistically assess the degree of correlation between the left and right arms, the Pearson product-moment Correlation Coefficient (PCC) was calculated. The PCC provides a measure of the linear correlation between two sets of data, where $PCC = 1$ refers to a total positive correlation while $PCC = 0$ indicates zero correlation between the data sets. Applying the Pearson test to the data for the subjects' left and right arms, the PCC was calculated to be 0.8240 with a *p-value* equal to $7.4564e - 07$ which is well below 0.05, indicating significantly high levels of correlation between the subjects' left and right arms.

Remark IV: *The level of correlation possibly associates with the level of similarities between the mechanical characteristics of the person's arms, despite existing muscle-strength variability as a result of the person's handedness. This association could be helpful in generating a map, based on which the* range of passivity/non-passivity degree for one arm of a person can be specified based on that of his/her other arm. Such a correlation map can be specially helpful in designing PDP controllers for applications involving bi-manual activities, e.g., in teleoperated robotics surgery. Nevertheless, this would require data collection from an extensive number of subjects in order to generate an accurate correlation map between the left and right arms, which is beyond the scope of this paper and will be the focus of future work.

4) Correlation Between Passivity/Non-Passivity Levels of the Arm and Physical Features of the Body: An interesting question to answer would be whether the passivity level of a person's arm can be associated with their physical features, e.g. weight and height. If so, a correlation map can be possibly generated, based on which the passivity level of a person's arm is estimated according to the person's physical features. In order to address this question, statistical analyses were conducted; and the level of correlation associated with the subjects' weight, height, arm length, and Body Mass Index (BMI) were
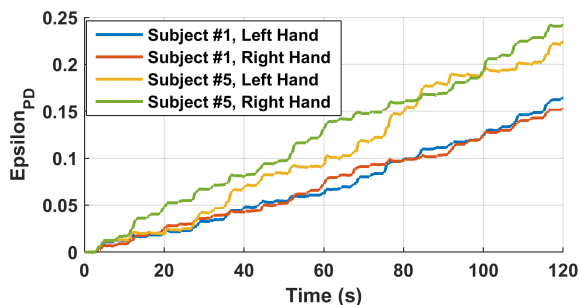
(a) ε_{PD} comparison between the left and right hands for subjects #1 and #5 during the low-frequency perturbation
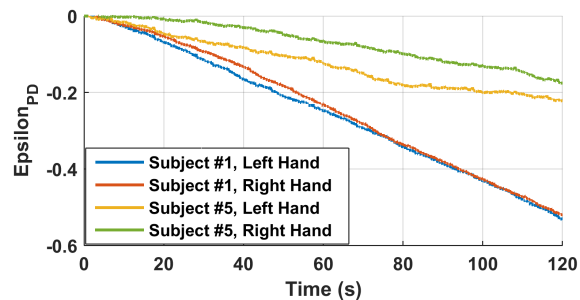
(b) ε_{PD} comparison between the left and right hands for subjects #1 and #5 during the high-frequency perturbation

Fig. 7: ε_{PD} comparison between the left and right hands for subjects #1 and #5

investigated. BMI is a quantified value derived based on one's weight and height ($BIM = \dfrac{Weight_{kg}}{Height_m^2}$), indicating the amount of tissue mass (muscle vs. fat). For this purpose, weight, height, and arm length of the participants were measured and recorded. Multiple statistical Pearson correlation tests were run for the data sets (physical features vs. passivity levels) to calculate the correlation level between each of the physical metrics (weight, height, arm length, and BMI) measured for the participants and the level of passivity of their arms; and the results are as follows: no significant correlation was observed between the subjects' height and the passivity levels of their arms during the low-frequency trials (*p-value*= 0.0744). A significant direct correlation of 0.7393 was, however, observed between the passivity level of their arms and their body weights (*p-value*= 0.0060). A significant direct correlation of 0.7563 was also observed between the subjects' BMI and the passivity level of their arms (*p-value*= 0.0044). This sounds reasonable, as the amount of tissue mass directly contributes to the mass and stiffness levels of an individual's arm.

Another effective factor could be the individual's arm length, which can affect the end-point impedance of his/her arm with respect to his/her arm impedances at the joints level. Therefore, the combination of the subjects' arm length (L_{Arm}) and their BMI was also tested ($L_{Arm} * BMI$), which resulted in significant direct correlation level of 0.7920 (*p-value*= 0.0021). Among all of the above, the latter metric provides the highest correlation, which can be used for the purpose of generating a correlation map that associates the physical features of an
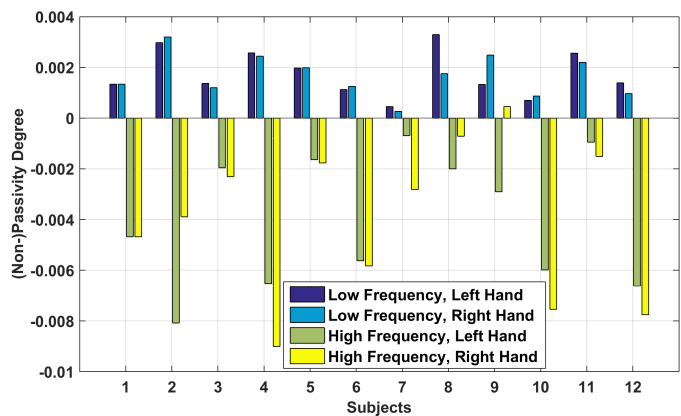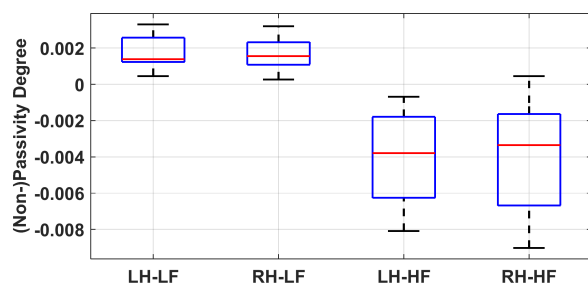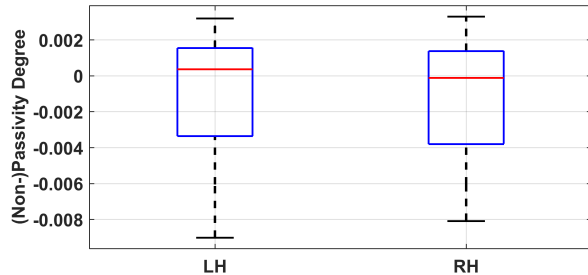

Fig. 8: Passivity/Non-passivity degrees for all the subjects calculated from the least-squared curves fitted to their ε_{PD}.

(a) The distribution of the passivity degrees for all the subjects during the four trials: LH-LF, RH-LF, LH-HF, RH-HF

(b) The distribution of the passivity degrees for the left hand (LH) and right hand (RH) of the subjects

Fig. 9: The distribution of the passivity/non-passivity degrees

individual to the passivity range of his/her arm. In order to generate an accurate association/correlation map, data collection and analysis should be carried out for a large number of subjects, which is beyond the scope of the current paper and will be the focus of our future work.

V. DISCUSSIONS

As elaborated earlier, the passivity of the human arm in the position-force domain, unlike in the velocity-force domain, is frequency-dependent and the operator arm may not remain passive for the high frequency ranges. Therefore, in order to develop position-force domain passivity controllers for

MM/SS systems, PD passivity of the operator should be also satisfied in addition to the PD passivity of the communication channel. PD passivity of the communication channel can be realized through the *conventional* passivity controllers in the literature by some change of variables [35]. The important issue, however, will be making the operator in the position-force domain passive for all frequency ranges. Development of an appropriate PD passivity controller for the operator in detail will be part of our future work. However, some of the possible solutions to this problem are briefly discussed below:

1) Filtering out frequencies above the natural frequency of the operator's arm. Considering that the frequency range characteristics of human motion is normally below their natural frequency, the higher frequency ranges of the signals flowing into the system may contain no significant contents. This, though, should be specifically discussed in the context of the application.

2) Virtually increasing the natural frequency of the operator's arm by adding positive stiffness (as a passivating element) into the system through the controller. This approach would be the dual of adding a damping term into the system in the conventional VD passivity controllers. The injection of the positive stiffness will shift the ε_{PD} to a higher level and, thereby, the combination of the virtual stiffness and the operator's arm can tolerate higher ranges of motion frequencies compared to the operator's arm alone. Although this approach can improve the high-frequency passivity of the system, it may degrade system performance in low-frequency ranges. Improving the arm PD passivity and, thereby, increasing the stability margin of a teleoperation system, by adding virtual stiffness at the operator side is interestingly in harmony with the stability condition derived in the literature for teleoperation systems based on the Small Gain Theorem [36].

3) Canceling out partially the effect of the mass of the operator's arm (the non-passivating element) by virtually injecting a negative mass into the system. This will decrease the total mass value of the combination of the operator's arm and the negative mass, increasing the natural frequency of the system and therefore shifting the boundary of passivity to higher frequency ranges. Unlike the virtual stiffness, the virtual mass will have a frequency-dependent effect on system performance, and will have a less degrading impact in the low-frequency range compared to that in high-frequency range.

Remark V: *The combination of the three suggested control approaches may be integrated into a PD passivity-observer/passivity-controller strategy, through which the passivity of the human arm terminal in position-force domain may be guaranteed. To what extent these strategies are helpful, along with other possible control strategies, requires further investigation and is a part of our future work.*

VI. CASE STUDY: PDP-BASED CONTROLLER FOR A BILATERAL SM/SS TELEOPERATION SYSTEM

As a proof of concept and in order to show the feasibility of the passivating approaches mentioned in the previous section,

simulations were run in PD for a haptics-enabled bilateral SM/SS teleoperation system. The dynamics parameters of the environment were set as $M_e = 1kg$, $B_e = 5N.s/m$ and $K_e = 150N/m$. The dynamics parameters operator's hand were also defined as $M_h = 1.5kg$, $B_h = 5N.s/m$ and $K_h = 100N/m$. The operator's exogenous force [23] was set as $f_h^*(t) = sin(t)$. The passivity measure ε_{PD} was calculated, indicating a passive terminal at the operator side. In order to induce non-passivity at the operator's arm terminal (to test the proposed passivating approaches), an additional force component was injected into the controller loop by augmenting the force generated at the environment side by $sin(5t)$, before feeding the environment force back to the operator's hand. Two of the passivating control approaches proposed in Section V were implemented, the results of which are discussed below:

Virtual Stiffness (VS): A virtual stiffness component was added at the arm terminal as a passivating controller. Three different values were set for this component and the resultant passivity measure were calculated at the arm terminal. Fig. 10 shows the resultant passivity measure before adding the controller $(VS = 0)$, and in the presence of three values $(VS = 30, 50, 70)$.●

Virtual Mass (VM): A similar procedure was repeated by adding negative virtual mass component at the arm terminal. Three different values were set for the MS control parameter as $(MS = -0.5, -0.7, -0.8)$ the result of which has been shown in Fig. 11.●

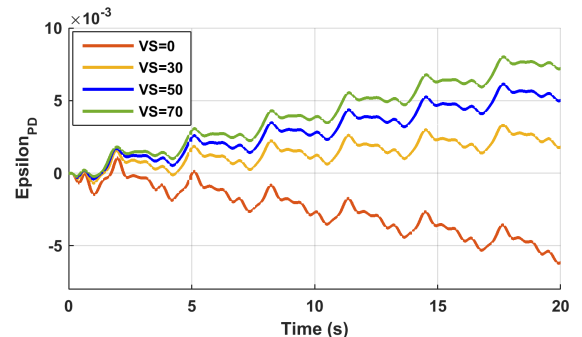Fig. 10: Passivity/Non-passivity measure at the arm terminal in the absence $(VS = 0)$ and in the presence of three various control parameters $(VS = 30, 50, 70)$.
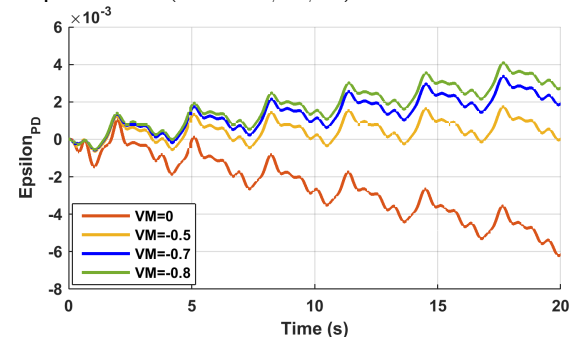

Fig. 11: Passivity/Non-passivity measure at the arm terminal in the absence $(VM = 0)$ and in the presence of three various control parameters (MS= -0.5, -0.7, -0.8).
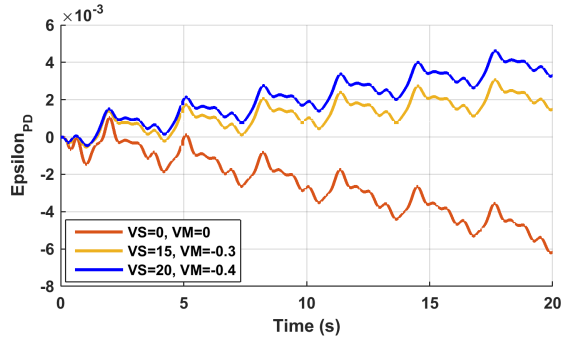
Fig. 12: Passivity measure at the arm terminal in the absence $(VS = 0, VM = 0)$ and in the presence of two various controller sets (VS=15, VM= -0.3 and VS=20, VM= -0.4).

Combination of Virtual Mass and Virtual Stiffness As the third scenario, a combination of VS and VM as the passivating controller was also evaluated. Two various sets of VS-VM was chosen $(VS = 15, VM = −0.3 and VS = 20, VM = −0.4)$. Fig. 12 shows the resultant PD passivity measure with and without $(VS = 0, VM = 0)$ the controller.•

As can be seen if Figs. 10-12, adding a positive VS component, or a negative VM component, or the combination of the two at the arm terminal can ensure PD passivatity of the operator's arm in a bilateral teleoperation system.

Fig. 13 compares force-tracking performance at the operator side in the presence of a VS controller vs. VM controller. To keep it comparable, the VM and the VS were chosen such that they have similar effects on the level of PD passivity of the arm terminal. Based on the results given in Figs 10 and 11, these controller parameters were chosen as $VM = −0.7$ and $VS = 30$, respectively. As can be seen in Fig. 13, the VM controller provided a better force-tracking performance and thereby, a higher level of transparency to the operator. To also quantify this, the Root-Mean-Square (RMS) of the force-tracking error was calculated for both cases, resulting in RMS error values of 0.0821 and 0.1446 for the VM and VS controllers, respectively.

VII. CONCLUSIONS AND FUTURE WORK

In this paper, the position-force domain passivity of the human arm was investigated in order to facilitate the development of passivity-based controllers in the position-force domain for teleopetarion systems. It was shown through mathematical analysis and experimental results that, unlike the velocity-force domain, the passivity of the human arm in position-force domain is frequency-dependent, and the operator does not remain passive in the position-force domain for all ranges of frequencies. User studies were conducted in support of the proposed hypothesis (frequency-dependent nature of the position-force domain passivity of the human arm), for the purpose of which 12 subjects were recruited. Each subject participated in four trials; data was collected for their both left and right arms for two different ranges of perturbation frequency. Statistical analysis was performed on the data for 48 trials to validate the proposed hypothesis. Statistical analysis was also conducted to study the correlation between 1) the levels of passivity of the left and the right arms of the subjects;
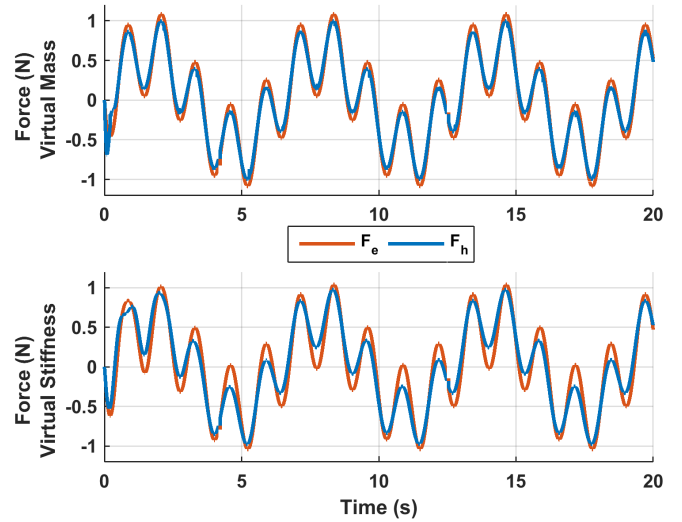

Fig. 13: Force-tracking performance in the presence of VM and VS controllers. F_e: desired force generated at the environment side; F_h: force applied to the operator's hand.

and 2) the level of correlation of the passivity of the subjects' arms and their physical characteristics, e.g., weight, height, and body mass index. Future work will focus on the development of correlation maps based on which the passivity level of an operator's arms can be specified using his/her physical characteristics. Integrating the passivity-based controllers in the literature with position-force domain passivity analysis, mainly with the focus on MM/SS teleoperation systems, will also be another aspect of our future work.

REFERENCES

[1] R. L'Orsa *et al.*, "Introduction to haptics for neurosurgeons," *Neurosurgery*, vol. 72, pp. A139–A153, 2013.

[2] J. Burgner *et al.*, "A telerobotic system for transnasal surgery," *IEEE/ASME Transactions on Mechatronics*, vol. 19, no. 3, pp. 996–1006, 2014.

[3] M. Shahbazi *et al.*, "A dual-user teleoperated system with virtual fixtures for robotic surgical training," in *IEEE International Conference on Robotics and Automation (ICRA)*. IEEE, 2013, pp. 3639–3644.

[4] M. Shahbazi *et al.*, "An expertise-oriented training framework for robotics-assisted surgery," in *IEEE International Conference on Robotics and Automation (ICRA)*. IEEE, 2014, pp. 5902–5907.

[5] P. R. Culmer *et al.*, "A control strategy for upper limb robotic rehabilitation with a dual robot system," *IEEE/ASME Transactions on Mechatronics*, vol. 15, no. 4, pp. 575–585, 2010.

[6] S. F. Atashzar *et al.*, "Networked teleoperation with non-passive environment: Application to tele-rehabilitation," in *IEEE/RSJ Int. Conf. on Intelligent Robots and Systems (IROS)*. IEEE, 2012, pp. 5125–5130.

[7] C. Melchiorri, "Robotic telemanipulation systems: An overview on control aspects," in *Proceedings of the 7th IFAC Symposium on Robot Control*, vol. 1, 2003, pp. 707–716.

[8] G. Salvietti *et al.*, "Multicontact bilateral telemanipulation with kinematic asymmetries," *IEEE/ASME Transactions on Mechatronics*, vol. 22, no. 1, pp. 445–456, 2017.

[9] R. J. Anderson and M. W. Spong, "Asymptotic stability for force reflecting teleoperators with time delay," *The International Journal of Robotics Research*, vol. 11, no. 2, pp. 135–149, 1992.

[10] A. Budak, *Passive and active network analysis and synthesis*. Waveland Press Inc, 1991.

[11] R. Lozano *et al.*, *Dissipative Systems Analysis and Control: Theory and Applications*. Springer Science & Business Media, 2013.

[12] P. F. Hokayem and M. W. Spong, "Bilateral teleoperation: An historical survey," *Automatica*, vol. 42, no. 12, pp. 2035–2057, 2006.

[13] A. Haddadi *et al.*, "Operator dynamics consideration for less conservative coupled stability condition in bilateral teleoperation," *IEEE/ASME Transactions on Mechatronics*, vol. 20, no. 5, pp. 2463–2475, 2015.

[14] V. Chawda and M. K. O'Malley, "Position synchronization in bilateral teleoperation under time-varying communication delays," *IEEE/ASME Transactions on Mechatronics*, vol. 20, no. 1, pp. 245–253, 2015.

[15] J.-H. Ryu *et al.*, "Stable teleoperation with time-domain passivity control," *IEEE Transactions on Robotics and Automation*, vol. 20, no. 2, pp. 365–373, 2004.

[16] R. J. Anderson and M. W. Spong, "Bilateral control of teleoperators with time delay," *IEEE Transactions on Automatic Control*, vol. 34, no. 5, pp. 494–501, 1989.

[17] G. Niemeyer and J.-J. E. Slotine, "Telemanipulation with time delays," *The Int. J. of Robotics Research*, vol. 23, no. 9, pp. 873–890, 2004.

[18] G. Niemeyer and J.-J. E. Slotine, "Towards force-reflecting teleoperation over the internet," in *IEEE International Conference on Robotics and Automation*, vol. 3. IEEE, 1998, pp. 1909–1915.

[19] N. Chopra *et al.*, "Bilateral teleoperation over the internet: the time varying delay problem," in *Proceedings of the American Control Conference, Denver, USA*, 2003.

[20] N. Chopra *et al.*, "On position tracking in bilateral teleoperation," in *Proc. of the American Cont. Conf.*, vol. 6. IEEE, 2004, pp. 5244–5249.

[21] J. Artigas *et al.*, "Position drift compensation in time domain passivity based teleoperation," in *IEEE/RSJ Int. Conf. on Intelligent Robots and Systems (IROS)*. IEEE, 2010, pp. 4250–4256.

[22] M. Shahbazi *et al.*, "A framework for supervised robotics-assisted mirror rehabilitation therapy," in *IEEE/RSJ International Conference on Intelligent Robots and Systems (IROS)*. IEEE, 2014, pp. 3567–3572.

[23] M. Shahbazi *et al.*, "Robotics-assisted mirror rehabilitation therapy: A therapist-in-the-loop assist-as-needed architecture," *IEEE/ASME Transactions on Mechatronics*, vol. 21, no. 4, pp. 1954–1965, 2016.

[24] G. Ganesh *et al.*, "Two is better than one: Physical interactions improve motor performance in humans," *Scientific Reports, Nature Publishing Group*, vol. 4: 3824, 2014.

[25] N. Hogan, "The mechanics of multi-joint posture and movement control," *Biological Cybernetics*, vol. 52, no. 5, pp. 315–331, 1985.

[26] F. A. Mussa-Ivaldi *et al.*, "Neural, mechanical, and geometric factors subserving arm posture in humans," *The Journal of Neuroscience*, vol. 5, no. 10, pp. 2732–2743, 1985.

[27] T. Tsuji *et al.*, "Human hand impedance characteristics during maintained posture," *Biological Cybern.*, vol. 72, no. 6, pp. 475–485, 1995.

[28] M. Dyck *et al.*, "Is the human operator in a teleoperation system passive?" in *World Haptics Conf. (WHC)*. IEEE, 2013, pp. 683–688.

[29] I. G. Polushin *et al.*, "A small gain framework for networked cooperative force-reflecting teleoperation," *Automatica*, vol. 49, no. 2, pp. 338–348, 2013.

[30] D.-H. Zhai and Y. Xia, "A novel switching-based control framework for improved task performance in teleoperation system with asymmetric time-varying delays," *IEEE transactions on cybernetics*, 2017.

[31] J. M. Dolan *et al.*, "Dynamic and loaded impedance components in the maintenance of human arm posture," *IEEE Transactions on Systems, Man and Cybernetics*, vol. 23, no. 3, pp. 698–709, 1993.

[32] T. Flash, "The control of hand equilibrium trajectories in multi-joint arm movements," *Biological cybernetics*, vol. 57, no. 4, pp. 257–274, 1987.

[33] N. Kottenstette and P. J. Antsaklis, "Relationships between positive real, passive dissipative, & positive systems," in *American Control Conference (ACC)*. IEEE, 2010, pp. 409–416.

[34] S. S. Haykin, *Active network theory*. Addison-Wesley, 1970, vol. 2680.

[35] M. Shahbazi *et al.*, "Networked dual-user teleoperation with time-varying authority adjustment: A wave variable approach," in *IEEE/ASME International Conference on Advanced Intelligent Mechatronics (AIM)*. IEEE, 2014, pp. 415–420.

[36] M. Shahbazi *et al.*, "Novel cooperative teleoperation framework: Multi-master/single-slave system," *IEEE/ASME Transactions on Mechatronics*, vol. 20, no. 4, pp. 1668–1679, 2015.

Mahya Shahbazi (S'10-M'17) is currently a postdoctoral research associate in the Department of Electrical and Computer Engineering at the University of Western Ontario (UWO), Canada and Canadian Surgical Technologies and Advanced Robotics (CSTAR). She received her Ph.D. degree in Electrical and Computer Engineering from UWO in January 2017. Mahya has been recipient of several awards including the 2014 highly competitive Ontario Graduate Scholarship (OGS). Her research interests include Medical Robotics, Telerobotics, Human-Robot Interaction, Artificial Intelligence, and Advanced Control Systems.

S. Farokh Atashzar (S'11-M'17) received his Ph.D. degree in Electrical and Computer Engineering from UWO, Canada, in 2016. Currently, Farokh is a postdoctoral research associate at CSTAR, Canada. During his Ph.D., Farokh received several awards including the OGS in 2013. His research broadly involves areas of medical robotics, physical human-robot interaction, bio-signal processing and advanced control systems.

Mahdi Tavakoli (M'08) is a Professor in the Department of Electrical and Computer Engineering, University of Alberta, Canada. He received his PhD degree in Electrical and Computer Engineering from UWO, Canada, in 2005. In 2006, he was a post-doctoral researcher at CSTAR, Canada. In 2007-2008, he was an NSERC Post-Doctoral Fellow at Harvard University, USA. His research interests broadly involve the areas of robotics and systems control. Specifically, his research focuses on haptics and teleoperation control, medical robotics, and image-guided surgery.

Rajni V. Patel (M'76-SM'80-F'92-LF'13) received his PhD degree in Electrical Engineering from the University of Cambridge, England, in 1973. He currently holds the position of Distinguished University Professor and Tier-1 Canada Research Chair in the Department of Electrical and Computer Engineering with cross appointments in the Departments of Surgery and Clinical Neurological Sciences, Schulich School of Medicine and Dentistry, UWO, Canada. He also serves as Director of Engineering at CSTAR.